Diseño de interfases de titanio poroso bioactivo para equilibrar las propiedades mecánicas y el comportamiento de las células *in vitro* hacia una mayor osteointegración

Estudiante
Raisa Juliana Pino Flórez

Director
Ana Fátima Civantos Fernández
(Juan José Pavón)

Codirector
José Antonio Rodríguez

FACULTAD DE CIENCIA Y BIOTECNOLOGÍA
UNIVERSIDAD CES
UNIVERSIDAD EIA
2019

Tabla de Contenido

1. INTRODUCCIÓN GENERAL

La necesidad de reemplazo de tejido óseo es una problemática mundial que se evidencia en estadísticas como las proporcionadas por la Asociación Dental americana, las cuales indican que 113 millones de norteamericanos adultos han perdido al menos un diente y que 109 millones de adultos mayores están desdentados (Crowninshield, R.D., Rosenberg, A.G., & Sporer, S.M., 2006).

En nuestro país, una investigación revelada por el IV Estudio Nacional de Salud Bucal (ENSAB IV), encontró que 6 de cada 10 colombianos les hace falta por lo menos una pieza dental y que el 33% de los mayores de 65 años han perdido todas sus piezas dentales. (Ministerio de salud y porteccion Social. Colombia, 2015).Estas pérdidas son generalmente asociadas a las condiciones de vida, las prácticas de cuidado y a enfermedades del sistema óseo; Por esta razón es frecuente el uso de implantes dentales.

En el desarrollo de implantes se necesita garantizar un balance adecuado entre propiedades mecánicas y biocompatibilidad, está última es bien proporcionada por el titanio (Ti) y sus aleaciones, y es por la cuál lo ha convertido en el biomaterial metálico de mayor éxito clínico para el remplazo de hueso. Sin embargo, la diferencia de módulo de elasticidad entre el Ti y el hueso receptor resulta en un fenómeno de apantallamiento de tensiones, produciendo reabsorción ósea alrededor del implante. (N. Sumitomo, K. Norikate, & T. Hattori, 2008). A pesar de su capacidad de osteointegración, el carácter bioinerte de la superficie del Ti produce una capa delgada de tejido fibroso, lo cual está muy relacionado con eventos de aflojamiento de los implantes. Esta problemática interfacial sumada con la incompatibilidad mecánica reflejada en los diferentes valores de módulo de Young, ha llevado a que gran cantidad de trabajos de investigación de los últimos 20 años estén enfocados a resolver este tipo de problemas. (Yadir Torres, Sheila Lascano, Jorge Bris, Juan Pavon, & Jose A Rodriguez, 2014) (Y. Torres, et al., 2012) (Juan Pavón., 2006)

Aunque se han logrado avances en ambos sentidos, algunos de ellos con aceptable éxito clínico, sigue existiendo la necesidad de investigar y desarrollar nuevos biomateriales base Ti que logren un balance ante la reabsorción ósea y la encapsulación, (M. Niinomi & M. Nakai, 2011) sin afectar de

manera significativa la resistencia mecánica de los implantes. El éxito de los implantes está ligado al mejoramiento de sus propiedades superficiales, (J.M Macak, et al., 2007) ya que la superficie estará en contacto directo y permanente con el medio vivo. Se ha encontrado que cultivos celulares *in vitro* aumentan su adhesión y proliferación con el cambio de la rugosidad en la superficie de un material, dando idea de que la modificación superficial de los materiales puede aumentar en gran medida la osteointegración; (Andrés O. Garzón, Nelly O, Aguirre, & Jhon J Olaya, 2013).

Con respecto a la topografía superficial del Ti para el mejoramiento de procesos de osteointegración del implante al hueso, diferentes estudios *in vitro* han mostrado que las rugosidades a escala micro, promueven la actividad celular. Existe un consenso en que algunos parámetros de rugosidad obtenidos mediante tratamientos mecánicos como el arenado al impactar superficies con un chorro de arena, resultan valores de rugosidad superficial de: altura media de picos, Ra = 4-5 µm, espacio medio entre picos, Pc = 65- 80 cm; donde estos valores promueven la adhesión de los osteoblastos, dando indicios de poder mejorar la osteointegración y, por tanto, disminuyendo el riesgo de aflojamiento de los implantes. (C. Aparicio, 2004).

La importancia de los aspectos cinéticos y jerárquicos de los tejidos, como sus diferentes escalas estructurales, desde lo macro hasta lo nano y-o molecular, (Shuilin Wu, et al., 2014). exigen una aproximación de diseño biomimético o bioinspirado que deben considerar estas premisas, por lo que el desarrollo de biomateriales implantables deben incluir escalas estructurales, técnicas de recubrimiento y modificación superficial que pueda mimetizar la matriz extracelular natural, donde se encuentran inmersas las células de los tejidos vivos, para así prolongar la vida útil de los dispositivos.

En este contexto, la búsqueda de nuevas alternativas que permitan ***redefinir*** algunas propiedades superficiales de Ti poroso que permitan reducir la reabsorción ósea, es uno de los principales objetivos de la investigación que se propone en este documento.

2. METODOLOGÍA

Las muestras iniciales de Ti poroso que se utilizaron en esta investigación, son el resultado de la optimización de la técnica de Pulvimetalurgía no convencional utilizando como espaciador bicarbonato de amonio (NH_4HCO_3), a través del control de la mezcla de polvos, compactación, disolución del espaciador y sinterización. Se utilizó la composición química de Ti grado IV acorde a la norma ASTM-37. Las muestras presentaron un balance óptimo de propiedades mecánicas, pues poseen módulo elástico semejante al hueso cortical, con las que se puede solventar el fenómeno de apantallamiento de tensiones. (Y.Torres, et al., 2014) (J. Pavon, et al., 2012) (J.A Rodriguez, et al., 2012)

Para la caracterización microestructural de las muestras, se evaluó la morfología superficial mediante microscopía electrónica de barrido **SEM-EDS** en un equipo JEOL JSM-6490LV. Adicionalmente, Con las imágenes obtenidas de microscopía metalográfica se hizo análisis de imagen con el software image j. Sobre estas muestras de Ti poroso con balance mécanico, se implementó un tratamiento químico con ácido fluorhídrico (HF) para exponer la superficie del sustrato y así eliminar la capa pasiva de óxido de titanio (TiO_2), adicionando un inhibidor orgánico complejo, el cual facilitó que el ataque químico fuera lo más homogéneo posible sobre la superficie y así evitar la pérdida excesiva de material*;* (Angel Coronel, 2015). La solución de HF e inhibidor se colocó en sus respectivos contenedores a baño termostático y se evaluaron diferentes tiempos de inmersión (0s, 125 y 625s) para las muestras

Para evaluar porosidad total e interconectada, además de medición de diámetro equivalente, tanto en muestras porosas, como en muestras macizas. Finalmente, dentro del proceso de caracterización, se utilizó microscopía confocal láser par evaluar los parámetros de rugosidad Sa, Sz y Sq que se obtuvieron con los tratamientos químicos en los poros del Ti.

Una vez obtenidas las muestras con su respectiva caracterización, se implementó la evaluación de las mismas de manera in vitro. Los nuevos biomateriales diseñados para futuro reemplazo óseo, se evalúan de manera *in*

vitro con cultivos celulares y luego de manera *in vivo* con animales. La evaluación *in vitro* usualmente utiliza líneas celulares; estás líneas permiten estandarizar el proceso de validación biológica, ya que otorgan fácil reproducibilidad y homogeneidad con el fin de reproducir resultados. Las líneas celulares que se usan con frecuencia en evaluar biomateriales para reemplazo óseos son las UMR-106, MBA-15 y MC3T3-E1.(M. Vandrovcova, & L. Bacakova, 2011)

Para evaluar la biocompatibilidad de las muestras de titanio con diferentes tamaño de poro y con parámetro de rugosidad modificados, se utilizaron las células C2C12-GFP, procedentes de la línea celular premioblástica de ratón C2C12, adquirida en ATCC (*American Type Culture Collection)*. Esta línea celular fue transfectada con un lentivirus para introducir proteína verde fluorescente (GFP) que expresa fluorescencia constitutivamente, la cual permite visualizar en tiempo real sus procesos de adhesión y proliferación a través de microscopía de fluoresencia invertida.

También se utilizó la línea celular pre-osteoblástica muscular MC3T3-E1, adquirida en ATCC (*American Type Culture Collection)*. Esta última línea celular es un buen modelo para estudiar los procesos de diferenciación y mineralización osteoblástica de manera *in vitro.* (Kanazawa I et al., 2007). Finalmente, se utilizó la línea celular RAW 264.7 (ATCC® TIB-71™), para evaluar la respuesta inmune provocada por los sustratos de Ti con nueva topografía superficial, ya que la evaluación del fenotipo de macrófagos después del contacto con las superficies de Ti es esencial en el diseño de implantes exitosos, pues los macrófagos tienen un papel clave en la aceptación del implante.

Las rutinas de subcultivo de las 2 líneas celulares MC3T3-E1 y las RAW 264.7 se realizaron en frascos de 75cm^2 con medio MEM de Dubelco (D6429, Sigma-Aldrich, St. Louis, MO). Para las C2C12-GFP se utilizó medio DMEM , ambos medios complementados con 10% de suero bovino fetal y un 1% de antibióticos de penicilina / estreptomicina (100U / mL, Invitrogen, Alemania).

Todas las muestras de Ti poroso se esterilizaron a 121ºC durante 30 minutos y seguidamente se introdujeron cuidadosamente en platos de 24 pozos para lavarlas con PBS y medio de cultivo, todo bajo condiciones estériles; Los

experimentos de actividad metabólica para las líneas C2C12-GFP y MC3T3-E1 y la tinción del citoesqueleto de esta última, se realizaron por triplicado en 4 puntos temporales (24h, 96h, 168h y 240h); con su respectivo blanco, correspondiente a medio sin células y muestras control de Ti macizo. Los experimentos de respuesta inmune de RAW 264.7 se realizaron después de 48 hr de siembra celular.

Las 3 líneas celulares se sembraron sobre los sustratos de Ti a una densidad inicial de 10.000 células/cm^2 . Se incubó durante 30 minutos y luego se adicionó 1ml de medio de cultivo, los platos de cultivo se sometieron a 37ºC y a una humedad de 5% CO_2 . Los cultivos de C2C12-GFP sobre los sustratos de Ti poroso, la evaluación morfológica de las MC3T3 y la polarización de las RAW 264.7 se visualizaron con ayuda de un microscopio de Fluorescencia (Olympus IX51).

Para los ensayos de actividad metábolica, se implementó la técnica de Alamar Blue, que es un método de reducción de resazurina. La resazurina (azul no fluorescente) es el principal compuesto del *Alamar blue* (*AB. Alamarblue® Cell Viability Reagent Invitrogen*). Este es reducido a resorufina (rosa altamente fluorescente) por óxido-reductasas que se encuentran principalmente en la mitocondria de células vivas. Así, la medida de fluorescencia obtenida de la resofurina es directamente proporcional a la cantidad de células vivas y es considerado un indicador de la función mitocondrial. Se añadieron 100 µl del reactivo AB directamente al medio de cultivo en una proporción 1:10, se incubó a 37°C, durante 1 hora 30 minutos en oscuridad; pasado este tiempo, cada una de las muestra se cambio cuidadosamente a un plato con nuevo medio de cultivo y se realizo la lectura de fluorescencia de los platos con AB (longitud de onda de excitación 570 nm y de emisión 590 nm).

En cuanto a la morfología celular de las MC3T3, Para cada punto temporal de cultivo de se hizo fijación de las células al sustrato. Se descarta el medio y los pocillos de cultivo se lavan 3 veces con PBS, posteriormente las células se fijan al sustrato con paraformaldehído al 4% durante 10min; nuevamente se hace lavado con PBS y se adiciona triton x-100 al 0.1% para permeabilizar la

membrana celular y pueda entrar el reactivo de Actina-Hoechst; siguiendo el protocolo comercial (Texas Red ^{R} X Phalloidin, Molecular Probes). Transcurridos 30 minutos de incubación en oscuridad a temperatura ambiente, se retiró el reactivo actina-hoetch, se realizaron dos lavados consecutivos con PBS y para visualizar en el microscopio de fluorescencia (Olympus IX51 microscope, filtro TRICT para actina y DAPI para hoechst, respectivamente) a cada muestras se le dio la vuelta dentro del plato de cultivo.

La detección de la actividad de la fosfatasa alcalina (ALP) se usó como un indicador de la diferenciación de MC3T3 preosteblástica hacia el linaje osteogénico. Después de 7 días de cultivo, las muestras se lavaron dos veces con PBS (500 µl) y se agregaron 100 µl / pocillo de tampón de lisis (Tris 50 mM, pH 6,8, Triton X-100 al 0,1%, MgCl2 2 mM). Se sembraron lisados celulares (20 µl) en una placa de 96 pocillos y se midió la medición de ALP utilizando 100 µl de fosfato de p-nitrofenilo en tampón 2-amino-2-metil-1-propanol (100 µl / pocillo). Después de 30 minutos de incubación a 37ºC en condiciones de oscuridad, la reacción se detuvo utilizando NaOH 0,5M (100 µl / pocillo) y se leyó la absorbancia a 450 nm utilizando un lector de microplacas (Synergy HT, Biotek).

Para el día 14, las células de osteoblastos se fijaron utilizando PFA al 4%, las muestras y posteriormente, se enjuagaron con un exceso de agua destilada (tres veces). Luego, muestras teñidas con rojo Sirio (Sigma, EE. UU.), Siguiendo el protocolo del fabricante. Brevemente, las muestras se lavaron dos veces con PBS, se tiñeron con una solución de tinción con alizarina S-red 40 mM (pH 4,2) y se incubaron a temperatura ambiente durante 20 minutos. Después de eso, la solución de tinción se eliminó y las muestras se enjuagaron con agua destilada tres veces, para finalmente identificarlas con un microscopio (Olympus, BX51).

El marcador de superficie CCR7 se estudió utilizando inmunocitoquímica para evaluar la polarización RAW 264.7. Los macrófagos cultivados se fijaron en paraformaldehído al 4% durante 20 minutos a temperatura ambiente y se incubaron durante la noche en una solución de bloqueo (suero de burro normal al 5%; triton X-100 al 0,3% en 1x PBS) a 4ºC. Después de bloquear la tinción no específica, se agregaron anticuerpos primarios, rata anti-CCR7 para la especificidad M1 (12 µg / ml, R&D Systems, MN). Luego, las células se incubaron con anticuerpo primario durante la noche y finalmente con anticuerpo

secundario, IgG anti-rata de cabra Alexa Fluor 350 (7 µg / ml, Thermo Fisher Scientific, MA) durante 2 horas a temperatura ambiente para CCR7. La visualización de las células marcadas con fluorescencia se realizó en un microscopio de fluorescencia invertido (Olympus IX51) con un filtro TRICT (λex / λem = 547/572 nm) utilizando el software de análisis CellD (Olympus).

3. Artículo(s)

Designing bioactive porous titanium interfaces to balance mechanical properties and in vitro cells behavior towards increased osseointegration

Ana Civantos[1,2,3], Cristina Domínguez[4,] Raisa Juliana Pino[5], Giulia Setti[3], Juan José Pavon[5], Enrique Martínez-Campos[3,6], Francisco Jose Garcia Garcia[7], Jose Antonio Rodriguez[4], Jean Paul Allain[1,2,8], Yadir Torres[4]

Designing bioactive porous titanium interfaces to balance mechanical properties and in vitro cells behavior towards increased osseointegration

Ana Civantos[1,2,3], Cristina Domínguez[4], Raisa Juliana Pino[5], Giulia Setti[3], Juan José Pavon[5], Enrique Martínez-Campos[3,6], Francisco Jose Garcia Garcia[7], Jose Antonio Rodriguez[4], Jean Paul Allain[1,2,8], Yadir Torres[4]*

[1]Department of Nuclear, Plasma and Radiological Engineering, College of Engineering, University of Illinois at Urbana-Champaign, USA
[2]Micro and Nanotechnology Laboratory, University of Illinois at Urbana-Champaign, USA
[3]Tissue Engineering Group, Institute of Biofunctional studies Complutense University of Madrid. Associated Unit to the Institute of Polymer Science and Technology (CSIC), Polymer Functionalization Group, Spain
[4]Department of Engineering and Materials Science and Transportation, University of Seville, Seville, Spain
[5]Group of Advanced Biomaterials and Regenerative Medicine, Bioengineering Program, University of Antioquia, Colombia
[6]Polymer Functionalization Group, Department of Applied Macromolecular Chemistry, Institute of Polymer Science and Technology, CSIC, Madrid, Spain
[7]Department of Inorganic Chemistry and Chemistry engineering, Instituto Universitario de Investigación en Química Fina y Nanoquímica IUIQFN, University of Cordoba, Spain.
[8]Department of Bioengineering, University of Illinois at Urbana-Champaign, USA

* **Corresponding author**:

Email: ancife@illinois.edu
Address: 1306, Micro and Nanotechnology laboratory, 104 South Wright Street. Urbana, Illinois 61801. USA
Phone: +1(217) 766-0951

Keywords: Porous titanium, Surface modification, Etching, Biomimetic scaffolds, Trabecular bone, Osseointegration.

ABSTRACT

Titanium implant failures are mainly related to stress shielding phenomenon and the poor cell interaction with host bone tissue. The development of bioactive and biomimetic Ti scaffolds for bone regeneration remains a challenge which needs the design of Ti implants

with enhanced osseointegration. In this context, 4 types of titanium samples were fabricated using conventional powder metallurgy (PM), named as fully dense (D), dense etched (DE), porous Ti (P) and porous etched Ti (PE). Porous (P and PE) samples were manufactured by space holder technique, using ammonium bicarbonate particles as spacer in three different ranges of particle size (100-200, 250-355 and 355-500 μm). Substrates were chemically etched by immersion in fluorhydric acid (HF) at different times (125 s and 625 s) and subsequently, were characterized from a micro-structural, topographical and mechanical point of view. Etched surfaces showed an additional roughness preferentially located inside pores. In vitro tests showed that all substrates were biocompatible (80% of cell viability), confirming cell adhesion of premioblastic cells. Similarly, osteoblast showed similar cell proliferation rates at 4 days, however, higher cell metabolic activity was observed in fully dense and dense etched surfaces at 7 days. In contrast, a significant increase of ALP expression was observed in porous and porous etched samples compared to control surfaces (dense and dense etched), noticing the suitable surface modification parameters (porosity and roughness) to improve cell differentiation. Furthermore, the presence of pores and rough surfaces of porous Ti substrates remarkably decreased macrophage activation reducing the M1 phenotype polarization as well CCR7 cell marker expression. Thus, a successful surface modification of porous Ti scaffolds has been performed towards a reduction on stress shielding phenomenon and enhancement of bone osseointegration, achieving a biomechanical and biofunctional equilibrium.

1. INTRODUCTION

Titanium (Ti) and some of its alloys are well recognized as the clinical grade metallic biomaterial with the best prognostic for bone replacement. However, the major issues associated with titanium implants failures are related to stress shielding phenomenon and lack of osseointegration. [1–3]. Many research studies have reported the biomechanical mismatch between Ti implants and the surrounding bone tissue, highlighting the higher elastic Young's modulus of Ti as the main cause associated with bone resorption and weakening of implants area. Under these circumstances, the implant may suffer micro-loosening and further combined with poor osseointegration will finally be rejected from the body [4].

Many efforts have been developed to create bioactive scaffolds with similar mechanical properties as bone tissue. Indeed, porous metallic biomaterials have become an interesting approach to reduce the stress shielding effect and to improve long-term fixation of Ti devices [4,5]. The porosity factor has been described before as a strategy to reduce the stress shielding effect due to reproducing similar stiffness and Young's modulus as native bone tissue. Several manufacturing techniques enable porous titanium scaffolds fabrication, such as freeze casting [6,7], rapid prototyping [8,9], laser processing [10,11], electric sintering [12–14], and powder metallurgy [15,16]. Unfortunately, many of those methodologies are complex processes and expensive, leaving toxic residues compromising their use in tissue reconstruction applications. Recently, powder metallurgy technology has been used with space holder (SH) particles offering an easy and scalable method to fabricate highly random interconnected pores with suitable mechanical properties [17,18]; The interconnected pores

are key factor in the development of healthy bone tissue since pores allow the required irrigation of blood and nutrients to feed the bone tissue in-growth. This SH technique has shown the advantage to control the space volume fraction which allows tailoring similar pore density and structure as cortical bone [16,19]. Earlier work showed similar Young's modulus values on porous samples (20 -28 GPa) as those of cortical bone (25GPa) using a variation in type and percentage of space holder [20,21] during processing. Although for bone regeneration certain stiffness and mechanical properties are required, according to literature, a pore size between 100 to 500 µm enhances vascularization process promoting tissue bone in-growth [22]. In addition, other studies also demonstrated that the pores generated by this space holder technique yielded intrinsic surface roughness along pore walls, improving the cell adhesion process and inhibiting bacteria attachment [23,24]. However, the increment of porosity may reduce the mechanical properties and compromise the internal stability of the implant which in turn can negatively affect in-vivo tissue reconstruction. In this context, the control of parameters such as pore size, pore volume fraction and pore morphology, as well as surface roughness are key factors to guarantee biomechanical and biofunctional stability with an enhancement in the osseointegration response in living bone tissue [25,26].

On the other hand, the inert biological character of titanium surfaces may lead low levels of cell interactions at the bio interface. This poor integration may delay or even impair the proper reconstruction of the damaged bone tissue, driving to the failure of the implant [27]. For this reason, it is essential to develop bioactive and biomimetic titanium surfaces, to promote the adhesion and differentiation of bone marrow mesenchymal stem cells, osteoblast, macrophages, and osteoclast recovering the required bone homeostasis [28].

Particularly, the implantation of any biomaterial implies an immune host response leading by the action of macrophages which are the first cell line in the immune response process [29]. As any biomaterial, Ti scaffolds triggers an inflammatory response, which usually is resolved in several days once the implant is integrated by the organism. In some scenarios, this initial inflammation may endure several weeks, evolving to a chronic inflammation response by encapsulating the Ti implant [30,31]. This fibrotic capsule isolates the metallic device within a thin layer of fibrous tissue, which reduces cellular interactions with native bone tissue and promotes bacterial infections. This complex and well-orchestrated reaction also referred to as foreign body reaction (FBR) is driven by macrophages, one of the first immune cells which arrive at the implantation area [32–34]. These immune cells are exposed to multiple signals (biophysical and chemical cues from both implant surface and the surrounding tissues). Depending on the integration of these signals, macrophages become activated exhibiting a wide spectrum of polarization states. [35] At either end of such a spectrum, M1 is commonly referred to pro-inflammatory phenotype and M2 to anti-inflammatory. Each M1 and M2 phenotypes show specific features, such as different cell surface markers; expression of particular genes; and secretion of specific cytokines, chemokines, and enzymes, as well as different cell shape [34].

Some reports have shown the importance of surface modification to successfully control macrophages response and enhance osteoblast cell differentiation [33,36,37]. Hence, surface treatments of porous Ti implants have been developed with the aim of controlling the inflammatory reaction and promoting cell differentiation by enhancing the biological interactions at the bio-interface. Chemical surface modification among other treatments such

anodic reaction, hydrogen peroxide, sol-gel, chemical vapor deposition, has contributed to the microtopography by increasing the roughness and the surface free energy, being both essential factors that affect cellular processes such as protein adsorption, cellular adhesion, migration, and differentiation [38]. However, it should be pointed out the great value of nanoscale order in the surface modification role to control cells behavior and develop biomimetic surfaces is still under research by some authors of this group (Civantos and Allain) which are working on the novel nanopatterning of porous titanium scaffolds.

As pointed out above, there is some evidence showing the benefits of porous and rough Ti surfaces in implant fixation and long-term stability [1,36]. Nevertheless, their combined effect has been poorly understood and their interactions with different cellular lineages have not been evaluated before with the aim to reproduce a bone in vitro environment. Under this premise, the hypothesis in this work, based on the controlled chemical etching modification of designed porous Ti disks, will be a biomimetic and bioactive strategy to reestablish bone homeostasis and support faster osseointegration. The mechanical properties and surfaces topography, such as porosity (pore size, shape, and distribution) and roughness profile, were characterized to evaluate their influence on premioblast, osteoblast and macrophage behavior. This study reveals a porous surface treatment as a successful approach to activate the porous Ti scaffolds which will enhance the osseointegration and fixation in bone tissue.

2. MATERIALS AND METHODS

2.1 Preparation of porous and rough Titanium samples

Ti porous samples were obtained by mixing 50% c.p. Ti powder grade VI (according to ATM F67-00), and 50% of ammonium bicarbonate (BA) as a space holder, with particle sizes between A: 100-200 μm, B: 250-355 μm. And C: 355-500 μm, previously obtained by sieving the spacer. After matrix compaction (800 MPa using a SUZPECAR 600KN), BA particles were removed in an oven in two steps (at 60 ºC and 110 ºC during 12 h each in low vacuum conditions). Finally, samples were sintered in a ceramic tube under high vacuum conditions (Carbolyte STF 15/75/450) at 1250 ºC during 2 at high vacuum conditions. Subsequently, the chemical etching treatment was performed using hydrofluoric acid (HF, 45 %) in distilled water (22 ml/l) and an organic inhibitor (0.5 ml/l). Samples were immersed in the solution at 50 ºC during two different times of exposure (125s and 625s). The etching times were chosen according to previous work by the authors (J.A. Rodríguez-Ortíz, et.al, 2015). Finally, the etched substrates were sonicated in distilled water and ethanol.

2.2 Titanium samples characterization

The surfaces of non-porous or fully dense (D), dense and etched (DE), porous (P) and porous and etched Ti samples (PE) were evaluated in relation to porosity parameters. Porosity index was measured following ASTM C373-88 by Archimedes' method, evaluating the density (ρ), total porosity (PT), and interconnected porosity (PI) [39] The porosity structure was studied by image analysis (IA), using a metallographic optic microscope NIKON EPIPHOT coupled to an RGB camera JENOPTIK PROGRESS C3. Images were analyzed by the software IMAGE-PRO PLUS 6.2. In terms of surface topography, a scanning electron microscopy (SEM, JSM-6490LV, Jeol, Japan), was performed at different magnifications. Confocal laser

microscopy (Sensofar S Neox), was employed to quantify the surface roughness, at the flat area and inside the pores.

In terms of macro-mechanical behavior, the non-etched and etched substrates were submitted in the uniaxial compression test (Instron 5505 universal testing machine) [40–43], in order to evaluate the Young's modulus (E) and the yield strength (σy) before and after the chemical etching. Additionally, substrates were characterized by dynamic Young's modulus (Ed) using ultrasound technique (KRAUTKRAMER USM 35 equipment) [44,45]. Otherwise, the micro-mechanical behavior was studied by Vickers micro-indentation at two different loads (HV0.3 and HV1), measuring 10 times per substrate type and load condition.

2.3 Cell culture

All these experiments were carried out in the facilities of Tissue Engineering Group (UCM). Ti samples were sterilized by autoclave at 121 ° C for 30 minutes and then carefully placed into 24 well-plates (Corning Costar). Then, cells were seeded onto the Ti substrates at different cell densities, depending on the cellular experiment. These experiments were performed in triplicate, and fully dense titanium (D), without pores and no chemical treatment, was used as the control sample (D0).

2.3.1 C2C12-GFP cell line

To study the cell biocompatibility of titanium samples, C2C12 premioblast mouse cell line, from American Type Culture Collection, (ATCC® CRL-1772™), was used. These adherent cells, previously transfected with a lentivirus to introduce green fluorescent protein (GFP) for expressing constitutively fluorescence, were cultured using DMEM (Dulbecco's Modified Eagle Medium, Sigma Aldrich), completed with 10 % fetal bovine serum (FBS) and 1% of Penicillin /streptomycin (100U / mL, Invitrogen, Germany). For adhesion and proliferation studies, cells were seeded at an initial density of 10,000 cells/cm2 during 24 and 96 h of incubation.

2.3.2. RAW 264.7 cell line

A mouse macrophage cell line, RAW 264.7 cells, (ATCC® TIB-71™), was used as a polarization model to evaluate the immune response induced by Ti substrates. RAW 264.7 cells were maintained in an undifferentiated state using Dulbecco's MEM (D6429, Sigma-Aldrich, St. Louis, MO), completed with 10 % fetal bovine serum (FBS) and 1% of Penicillin /streptomycin (100U / mL, Invitrogen, Germany). Cell passages were performed at 80% of cell confluence in 75 cm2 using cell scrapers. Immune response experiments were run after 48h of cell seeding at a density of 10.000 cells per cm2.

2.3.3. MC3T3-E1 cell line

MC3T3-E1 pre-osteoblastic cell line (ATCC CRL-2593), was employed to reproduce the bone tissue environment. This cell line is a suitable model for studying osteoblastic differentiation in vitro. The subculture routing was performed in MEM (Minimum essential medium, Sigma Aldrich, Germany), completed with 10 % fetal bovine serum (FBS) and 1%

of Penicillin /streptomycin (100U / mL, Invitrogen, Germany) and culture flasks were placed in a humid atmosphere with 5% CO2 and at 37 ºC. For differentiation and mineralization cell studies, culture media was enriched with ß-glycerophosphate (50 mM), Ascorbic acid (10 mM) and Dexamethasone (10 nM), seeding 5000 cells / cm2 (changing media every two-three days) and analyzing at 7 and 14 days respectively.

2.4 Cell Adhesion and proliferation assays

Attachment and proliferation of C2C12-GFP were analyzed by inverted fluorescence microscopy (Olympus IX51) and CellD Software (Olympus). Cell metabolic measurement was measured to evaluate the cell adhesion on day 1. To that end, AlamarBlue assay (DAL1100, Thermofisher, USA) was performed following the manufacturer's instructions. Assays were carried out by triplicate for each sample condition. This non-toxic and scalable method uses the natural reducing power of living cells, generating a quantitative measure of cell viability and cytotoxicity. Briefly, samples previously seeded with cells were placed in new 24-well plates and added 10% of the culture volume of AlamarBlue dye. After 90 mins of incubation, fluorescence signal, with an excitation wavelength of 530 nm and an emission wavelength of 590 nm, was read in a microplate reader (Synergy HT, Biotek). Cell adhesion experiments were evaluated at 1 day and proliferation studies at 4 and 7 days for C2C12-GFP and MC3T3E1 respectively.

2.5 Cellular morphology evaluation

For each culture time point, cells were fixed with 4% paraformaldehyde (PFA) solution during 15 min. Afterward, titanium samples were rinsed carefully with PBS twice and permeabilized with 0.1% (v/v) Triton X-100. Subsequently, samples were washed with PBS and the actin cytoskeleton was stained with Texas Red®-X phalloidin (Molecular Probes), for 20 minutes at room temperature (RT) and in darkness. As a contrast marker, cell nuclei were stained using Hoechst (Invitrogen, Molecular Probes). Samples were observed using an inverted fluorescence microscope (Olympus IX51) with a TRICT filter (λex/λem=550/600 nm) for Actin, and DAPI filter for Hoechst (λex/λem = 380/455nm) and images were treated by CellD analysis software (Olympus).

2.6 Immunocytochemistry for immune response analysis

CCR7 surface marker was studied using immunocytochemistry in order to evaluate RAW 264.7 polarization. Cultured macrophages were fixed in 4% paraformaldehyde for 20 min at RT and incubated overnight in a blocking solution (5% Normal Donkey Serum; 0.3% Triton X-100 in 1x PBS) at 4ºC. After blocking non-specific staining, primary antibodies were added, rat anti-CCR7 for M1 specificity (12 µg/ml, R&D Systems, MN). Then, cells were incubated with primary antibody overnight and finally with secondary antibody, Alexa Fluor 350 goat anti-rat IgG (7 µg/ml, Thermo Fisher Scientific, MA) for 2 hours at RT for CCR7. The visualization of the fluorescent-labeled cells was performed in an inverted fluorescence microscope (Olympus IX51) with a TRICT filter (λex/λem=547/572 nm) using CellD analysis software (Olympus).

2.7 Cell differentiation: ALP measurement

The detection of alkaline phosphatase (ALP) activity was used as an indicator of pre-osteoblastic MC3T3 differentiation towards osteogenic lineage. After 7 days of culture, samples were washed twice with PBS (500 µl), and 100 µl/well of lysis buffer (50 mM Tris pH 6.8, 0.1% Triton X-100, 2 mM MgCl2) was added. Cell lysates (20 µl) were plated in a 96 well plate and ALP measurement was assayed using 100 µl of p-nitrophenyl phosphate in 2-amino-2-methyl-1-propanol buffer (100 µl/well). After 30 mins of incubation at 37ºC in dark conditions, the reaction was stopped using NaOH 0.5M (100 µl/well), and the absorbance at 450 nm was read using a microplate reader (Synergy HT, Biotek).

2.8 Cell mineralization: Alizarin red assay

At day 14, osteoblast cells were fixated using PFA 4%, samples and subsequently were rinsed with an excess of distilled water (three times). Then, samples stained with Sirius red (Sigma, USA), following manufacturer's protocol. Briefly, samples were washed twice with PBS, stained with 40-mM alizarin S-red staining solution (pH 4.2) and incubated at RT during 20 mins. After that, the staining solution was removed, and samples were rinsed with distilled water three times, to finally be identified by microscope (Olympus, BX51,).

2.9 Statistical analysis

Statistical analysis was performed using Origin Pro software expressing results as mean ± standard deviation. Macrophages and osteoblast experiments were performed in triplicate. Statistical significance was obtained and expressed as * $p < 0.05$.

3. RESULTS AND DISCUSSION

3.1. Preferential etching process inside pores

The presence of pores can promote cellular adhesion on the substrates. In this context, it is important to characterize the sample porosity, in order to study its influence in biological behavior. Non-etched porous substrates (A0, B0, and C0) presented a PT results, from Archimedes' method and IA, closed to 50 % (criteria design), as shown in Table 1. This result validates the space holder technique as a fabrication process to tailor the desired porosity in Titanium-based substrates. Nevertheless, there are some differences among samples values, being those of IA slightly greater than Archimedes' method ones. The main reason is that IA is focused on the substrate surface while Archimedes' method is a volumetric technique. However, in any case, both methodologies follow the same trend, obtaining greater porosity for bigger ranges of pore size (C0). It is interesting to mention that the D sample also presented a low porosity, showing very small pores (Deq smaller than 5 μm) as a consequence of the powder metallurgy process. In general, the Deq of pores generated by the spacer particles reached a value between the range of the spacer particle size, fixed by the design criteria. In terms of interconnected porosity, it is remarkable that almost all pores of

porous substrates were interconnected, potentially enhancing the bone in-growth through the implant.

After substrates etching, PT increases for all samples types, especially at etching time of 625 seconds (Table 1). It is worth mentioning the □PT for C625 (8.4 %), a very high value compared to the rest of substrates. The reason is that pore size is bigger, making it easier for the acid solution to cross the entire sample. Furthermore, the interconnected pores experiment also demonstrated a significant size increase in relation to non-etched substrates (Table 1).

Figure 1 shows the SEM images of all Ti surfaces including, the macroscopic view in the upper insets. In terms of pore size, in non-modified substrates (P0) the spacer particles determined the range of pore size during the fabrication process as it is observed in Fig. 1. As expected, increasing the Deq of pores, there is a reduced number of pores per area, showing greater Ti matrix between them. In addition, as size of the pores increases, a morphology with higher irregularity is exposed. Higher magnifications of A0, B0 and C0 pores (Figure 2) revealed some roughness patterns inside the pore walls due to the PM process. These patterns, as well as the presence of pores, results in a greater surface area when compared to D0, and therefore, cells find a higher active surface area to attach.

Once the substrates were chemically etched, the microstructural and mechanical properties also changed, compromising the stability and functional balance of the implant. Visually, it is appreciable that the color of substrates darkens, loosening the polished metal bright (Figure 1). The substrate topography is also highly modified after the etching within 125 and 625 seconds, as observed in SEM images of Fig. 1. Figure 2 presents at higher magnifications the

effect of HF on flat surface between pores and inside pores surfaces. It was unexpected the appearance of a new roughness pattern generated during the etching, based on geometrical features on all surfaces, simulating stings (see Figure S1 of Supporting Information and the upper insets in Fig. 3). These features increased in terms of number and size (about 10 to 20 nm) in all porous substrates at 625 s. As expected, etched fully dense surfaces (DE125 and DE625) presented a lower density of geometrical features compared to PE surfaces. As a result, confocal laser allowed to obtain the main roughness parameters (Sa, Sq and Sz) for all samples (Table 1).

Regarding roughness values (Sa) corresponding to flat surfaces (shown in Figure 3 and in detail in the upper insets), 625 s of etching time reached the highest Sa values in B (10.36 µm) and C (9.53 µm) samples compared to their counterparts DE (5.05 µm) and A (5.23 µm) surfaces. Therefore, the acid treatment presented a stronger effect on bigger pores on flat surfaces. This trend was also observed at pore surfaces, getting a higher modification on B625 with more pores and bigger size than A samples, followed by C625, with a lower number of pores but the highest size. In general, the chemical modification achieved a pronounced increase of roughness values, highlighting 625 s as the highest Sa obtained (47.11 µm, 71.84 µm, and 47.18 µm for A, B, and C respectively). Therefore, the chemical etching process showed a homogeneous modification with higher affinity for the surface inside pores than outside (flat areas) of the PE samples, which was also correlated with an increment of pore size and pore interconnectivity (see Fig. 1 and S1 of supporting information). These Sa results were in accordance with the Sa reported by other authors[46–49]. For example, Conrado and coworkers correlated the used of sandblasting treatment to

obtain roughness values for Ti flat surfaces of 7 μm (Sa), which indeed promoted an enhancement of osteoblast differentiation. [50]. The increase in roughness values by chemical treatment and by anodizing (electrochemical modification) have been correlated to an increased surface area, improving cell adhesion and differentiation process [51,52].

As mention before, the presence of pores reduces Young's modulus of titanium substrates, as well as other mechanical properties, which could compromise the biomechanical equilibrium of implants. In this context, it is essential to study the macro (uniaxial compression test and US) and micro-mechanical behavior (Vickers micro-hardness). Table 2 shows the Young's modulus (E) and strength yield (σy) for all substrates, as well as dynamic Young's modulus (Ed). All values for non-etched porous substrates were close to those of the cortical bone (Young's modulus of 20–25 GPa and mechanical strength of 150–180 MPa) for porous substrates, guaranteeing good mechanical behavior. In terms of micro-mechanical behavior, micro-hardness values were higher for HV0.3 than for HV1 for all types of substrate, as a consequence of indentation size and localized micro-plasticity phenomena effects. The micro-hardness of porous substrates is closed to that of D for HV0.3 (377), due to the matrix between pores is large enough, having a similar behavior to fully dense substrates. However, while for greater loads (HV1) the D results were similar to that of HV0.3 (342), values decreased because of the pores influence, being lower as pore size increased.

The increase of substrate porosity after chemical etching results in a decrease of mechanical properties due to a slight loss of structural integrity. In general, E decreased for samples after the etching in comparison to non-etched substrates, as a consequence of PT increase (Table

2). Otherwise, the trend of σy depends mainly on pore size, showing lower values as pore Deq is greater. Related to that, it is remarkable that σy decrease more drastically for substrates with the biggest pore size (C), due to the acid solution reaching deeper into the porous titanium samples.

3.2 Enhanced cell attachment and proliferation of micro-rough and porous Ti scaffolds.

Size, morphology and pore distribution, as well as a surface modification with HF of c.p.Ti samples are considered key factors in cellular response. For that reason, C2C12-GFP, a murine premioblast cell line, was used to evaluate cell viability at 1 day. Figure 4 showed cell viability results for all c.p. Ti surfaces, expressed in percentage. All substrates reached more than 80% of cell viability compared to cells growing on D0. Neither BA size and morphology particles nor HF time treatment produced significative differences at p 0.05 level, which means that a short time period, the cell viability was influenced by neither those factors. In addition, the presence of the GFP group allowed tracking the cell culture by inverted fluorescent microscopy. Figure 5 showed the compiling fluorescence microphotographs of C2C12-GFP cells in adhesion and proliferation states at 1 and 4 days of cell culture. All c.p. Ti surfaces were biocompatible, which allowed the proper cell adhesion and proliferation over time. At day 1, D0 was the only substrate which showed a higher number of attached cells which correlated the increased cell metabolic activity (see Fig.5A and Fig. 4 respectively). However, at 4 days of cell culture, all surfaces supported similar cell proliferation covering the entire surface and even pore walls (Fig. 5B).

Several studies have reported that the topography, chemistry, and surface energy of metallic-based biomaterials influence the initial adhesion and differentiation of osteoblastic lineage cells. These results agree to those reported in other studies [27,53]. This cell behavior has been evaluated by Chang and co-workers growing mesenchymal stem cells onto 70% of porous Ti surfaces. Although the initial attachment was showing low cell density at 24h, cells could migrate and proliferate increasing cell density at 4 days of incubation [53], similar to results reported here. All samples have shown cytocompatibility with premioblastic C2C12-GFP model. Etched samples showed similar cell density as non-etched, allowing cells to attach and proliferate, and suggesting that neither pore and chemical modification did not diminish cell affinity. In general, the entire surface of all substrates was totally covered by premioblastic cells, highlighting the presence of C2C12-GFP cells inside pores and following pore edges. In these fluorescent images, cells presented a similar elongated morphology on flat surfaces and on pores samples, confirming the suitable surfaces for cell proliferation purposes.

3.3 Porous and etched Ti surfaces improves osteoblast cells adhesion and proliferation.

After preliminary biocompatibility evaluation of c.p. Ti samples, a murine preosteoblastic cell line MC3T3-E1 was used to further analyze the interactions with specific bone cells. **Figure 6** showed the cell metabolic activity at 4 and 7 days of cell culture (A and B respectively). In Fig.6A, cell metabolic levels were similar for all surfaces ($p \geq 0.05$), although it was observed a trend of higher metabolic activity on etched surfaces and even more on 625 s of treatment. At day 7, significant statistic differences on osteoblast cell proliferation (* $p \leq 0.05$) were observed for non-porous samples compared to P and PE (Fig. 6B). Indeed, the

strongest significant differences were observed for D0 and D125 compared to the rest of the surfaces (*p≤0.05). It should be noticed that pore size did not achieve a reduction of AlamarBlue fluorescence levels for each group, observing similar metabolic activity among all P and PE substrates. In contrast, the HF modification showed a reduction in osteoblast proliferation, as lower fluorescence levels for 125 and even more, for 625 seconds were observed.

Osteoblastic cell behavior in non-porous substrates (D0, DE125, and DE 625) was similar to those reported in previous studies, in which the metabolic activity of osteoblast during adhesion and cell proliferation process were higher on smooth than kinetic rough surface [27,54]. Chen and coworkers evaluated the MG63 osteoblast cell adhesion onto porous Ti surfaces at 24 h by MTT. Cell viability was similar between three different porosity volume fractions (30%, 40%, and 70%) and three sizes of spacer particles, showing no statistical differences between them.

MC3T3 cells present complex cellular machinery involved in proliferation and differentiation process which influence the cell metabolic in both states. Surface features have shown not only to influence the adhesion but also differentiation of osteoblastic cells, showing a reduction of proliferation rate in regard to increasing production of bone matrix proteins including ALP, collagen, osteopontin, and osteocalcin [54,55]. Regarding other cellular processes affected by roughness treatment, protein adsorption or hemocompatibility can be improved by means of surface modification, particularly increase in surface roughness, in bone and vascular tissue regeneration [56,57]. Romero and Gavilan (2017) evaluated the protein layer adhered onto Ti smooth surfaces, observing an increase in the

number of proteins related to glycolysis and apoptosis (such proteins of the complement system, C3), whereas Ti rough surfaces showed an increased in cell signaling pathway by integrin and blood coagulation process (Apo E, and antithrombin). This roughness modification confirmed the effect on cell adhesion and the higher cell metabolic levels observed on flat Ti surfaces [56].

As a result of low cell metabolic activity, it could be expected a reduction of cell density. However, cell morphology evaluation through cytoskeleton and nuclei staining after 7 days of cell culture revealed similar cell density for all substrates (**Figure 7**). Furthermore, samples were completely covered by cells on flat and within pores surfaces. The higher cell density presented on D samples hindered the analysis of osteoblast morphology, thus, the organization of F-actin fibers evaluation was only performed on P and PE surfaces. Flat surfaces on P (A0, B0, and C0) showed similar cell density and a well-spread cell cytoskeleton with a polygonal shape morphology. When surfaces were etched, the osteoblast started to feel the topography and adjust to it a more cuboidal cell shape. Nevertheless, the increase on the surface area of P and PE samples showed cells attached on pore walls, which correspond to unfocused cell nuclei (blue dots that are far away to focus properly using inverted fluorescence microscopy). This cell morphology was also observed on C2C12-GFP, highlighting an elongated cell shape, displayed a fusiform morphology, following pores edge and growing on flat surfaces. In contrast, these cells displayed a cuboidal or rounded shape inside the pores.

These cells presented an elongated fibroblastic cell morphology, which has been reported by several studies to an advanced cell adhesion state [58] (Fig. 5A). P and PE samples noticed lower C2C12-GFP cells, with rounded shape even inside pores which correspond to unfocused green dots. In addition, it should be noticed the cell orientation observed on DE samples as a response to the rough topography developed by the etching process. The micro-roughness patterns guided cells growth with a certain orientation, as it was observed in DE125 and DE625. In contrast, this cell distribution and orientation were random on fully dense substrates, as observed after C2C12-GFP and MC3T3 cell lines results (see Fig. 5B and Fig.7). Similarly, the presence of pores and etched roughness favored a random distribution of osteoblasts cells as D0 samples (Fig. 7).

3.4 Porous and etched Ti surfaces promotes osteoblast cells differentiation.

Figure 8 showed the results of alkaline phosphatase enzyme (ALP) quantified at 7days. MC3T3E1 cells, cultured in osteogenic media, showed higher levels of ALP in all P and PE samples compared to non-porous Ti samples (D0), and also, non-etched control surfaces (DE125 and DE625) with significant differences ($*p \leq 0.05$). Indeed, D0 without pores and any surface modification showed the lowest ALP levels, thus, porous and rough surfaces had a synergy effect on cell differentiation, which was confirmed finding the highest values for PE 625. On the other hand. the size and pore morphology did not show a significant increase of ALP expression, however, there was a clear trend with higher ALP levels on etched bigger pores (C125 and C625). Alkaline phosphatase expression showed an early upward trend in rough and porous samples in comparison to smooth surfaces. Moreover, C samples reached

higher levels of this bone marker expression. These results are in agreement to those reported in the literature. Indeed, Li et al analyzed the ALP activity at 7 days of human bone marrow mesenchymal stem cells (hBMMSCs) onto porous Ti6Al4V scaffolds, in which they showed an increased absorbance at 405 nm for porous substrates with 400-500 μm of pore size. [55] **Figure 9** showed cell mineralization results which revealed an increase in calcium deposits for P and PE samples compared to D0 and D125 surfaces. Taking into account the presence of calcium deposits over these samples, an optimal osteoblastic behavior is suggested. Although a more complex study, including other mid and late expression markers (osteocalcin, bone sialoprotein…), is needed, sample treatment did not decrease bone differentiation over all surfaces. Thus, the roughness parameter by itself had a clear effect on cell differentiation at earlier stages of osteoblast incubation as it is observed between D substrates (0, 125, and 625) and PE125 and PE625s. This improvement of cell differentiation and mineralization are in agreement to those values reported in similar studies highlighting the role of micro-roughness surfaces as the activator to induce these cellular processes. [1,27,59,60]

3.3 Reduced M1 polarization in bioactive porous Ti

The evaluation of macrophages phenotype after contact with the Ti surfaces is essential in the design of successful implants since macrophages have a key role on the acceptance of the implant. In order to study the influence of porous and etched surfaces, RAW 264.7 cells were seeded on samples during 48h of cell culture, to evaluate cell morphology and specific cell markers related to the M1 phenotype. As it is shown in Figure 10, macrophages growing on D0 presented an increased polarization of M1 phenotype which was corroborated by the

presence of macrophages with several nuclei inside, starry cell shape and bigger in size than non-activated macrophages. This M1 phenotype observed on non-porous and non-etched surfaces (D0) was also confirmed by the positive signal of CCR7 immunostaining. In contrast, macrophages in contact with porous non-etched samples (A0) showed a round cell shape similar to the specific cell morphology that was found in TCP control and the other c.p. Ti sample. Moreover, the tendency of the activation of macrophages decreased when substrates presented porous and etched surfaces, such as DE625, and A625. In these modified samples, it was not possible to detect large multinucleated cells that could differentiate into FBGC, as it was observed on D0 samples. Indeed, A625s sample (small pores size and higher roughness values) showed less M1 polarization at the same time of cell incubation than DE625. It is noteworthy to mention great influence of surface properties on the immune cell response mediated by macrophages, confirming the potential benefits of porosity and roughness on Ti-based materials to reduce the M1 phenotype activation which is not desired on bone tissue reconstruction purposes and therefore, the lack of M1 promote fa faster healing Process and the presence of pores the neovascularization required for the new bone tissue.

4. CONCLUSIONS

In this work, it has been developed a chemical treatment of porous c.p.Ti surfaces to modify the roughness in a controlled manner by using an organic inhibitor to generate the observed additional micro-roughness. The etching treatment modified substrates surfaces, as well as porosity in terms of volume fraction and morphology. All this micro-structural and topographical variations involved a decrease of substrates mechanical properties, getting

values closed to those of cortical bone, confirming more biomimetic porous ti scaffolds. This study correlates cell viability, adhesion, proliferation, cell morphology and immune response of premioblastic cells, pre-osteoblastic cells, and macrophages. Cell differentiation was improved, and the immune response was controlled to reduce M1 phenotype. Samples with the time of the attack of 0s and 125s favored the biocompatibility of the samples, whereas the samples with the chemical attack of 625s enhanced the processes of osteoblast differentiation. In vitro evaluation of porous Ti samples is not sufficient to determine the degree of osseointegration of the samples; making necessary in vivo studies with animal models that allow a better understanding of osseointegration processes in the complex environment.

5. ACKNOWLEDGEMENTS

This article is also dedicated to our dear friend and colleague Prof. Juan Jose Pavón, who prematurely passed away early in 2017, his dedication to his work, his students, his friends and family, will always be remembered. This work was supported by the Ministry of Economy and Competitiveness of Spain under the grant MAT2015-71284-P and of the Junta de Andalucía – FEDER (Spain) through the Project Ref. P12-TEP-1401. The authors would like to thank technician J. Pinto for assistance in micro-mechanical testing.

APENDIX A. Supporting information

6. REFERENCES

Andrés O. Garzón, Nelly O, Aguirre, & Jhon J Olaya. (2013). Estado del arte en biocompatibilidad de recubrimientos. *Visión Electrónica*, *Volumen:7,* pág: 160–177.

Angel Coronel. (2015). *Surface Modification of Porous Titanium for Bone Repair: Controlled Etching and Deposition of Bioactive Composite Coatings by EPD Technique* (Pregrado). Universidad de Sevilla.

C. Aparicio. (2004). *Tratamientos de superficie sobre Ti Cp para la mejora de osteointegración de los implantes dentales.* Universidad Politecnica de Cataluña.

Crowninshield, R.D., Rosenberg, A.G., & Sporer, S.M. (2006). Changing demographics of patients with total joint replacement. *Clinical Orthopaedics and Related Research*, 266–272.

J.M Macak, H Tsuchiya, , A. Ghicov, K. Yasuda, R. Hahn, & S. Bauer. (2007). TiO2 nanotubes: Self-organized electrochemical formation, properties and applications, *11*(1–2,), Pages 3-18.

Juan Pavón. (2006). *Fractura y fatiga por contacto de recubrimientos de vidrio sobre Ti6Al4V para aplicaciones biomédicas*. Universitat Politècnica de Catalunya. Departament de Ciència dels Materials i Enginyeria Metal·lúrgica.

Kanazawa I, Yamaguchi T, Yano S, Yamahuchi M, Yamamoto M, & Sugimoto T. (2007). Adiponectin and AMP kinase activator stimulate proliferation, differentiation, and mineralization of osteoblastic MC3T3-E1 cells. *BMC Cell Biology*, *8: 51*.

M. Niinomi, & M. Nakai. (2011). Titanium-Based Biomaterials for Preventing Stress Shielding between Implant Devices and Bone. *Internacional Journal of Biomaterials*, 1–10.

M. Vandrovcova1, 1, & L. Bacakova. (2011). Adhesion, growth and differentiation of osteoblasts on surface-modified materials developed for bone implants. *Physiol Res. .*, ;*60(3):*, 403-17.

Ministerio de salud y porteccion Social. Colombia. (2015). IV Estudio Nacional de Salud Bucal. ENSAB IV. Situación en salud Bucal. Retrieved from https://www.minsalud.gov.co/sites/rid/Lists/BibliotecaDigital/RIDE/VS/PP/ENSAB-IV-Situacion-Bucal-Actual.pdf

N. Sumitomo, K. Norikate, & T. Hattori. (2008). Experiment study on fracture fixation with low rigidity titanium alloy: plate fixation of tibia fracture model in rabbit. *Journal of Materials Science*, *19. No. 4*, 1581–1586.

Robinson Montes. (2013). *Desarrollo de nuevas superficies de Ti vìa electroquìmica para implantes dentales.* Universidad de Antioquia.

Y torres, J. Pavon, & JA Rodriguez. (2012). Processing and characterization of porous titanium for implatns. *Journal of Materials Processing Technology*, 1061–1069.

Y. Torres, J.A Rodriguez, J.Pavón, S. Arias, M. Echeverry,, S. Robledo, & V. Amigo. (2012). Processing, characterization and biological testing of porous titanium obtained by space-holder technique. *J Mater Sci.*, 6565-76.

Yadir Torres, Sheila Lascano, Jorge Bris, Juan Pavon, & Jose A Rodriguez. (2014). Development of porous titanium for biomedical applications: A comparison

between loose sintering and space holder techniques. *Materials Science and Engineering C 37*, 148–155.

Y.Torres, P.Trueba, J.Pavón, I. Montealegre, & J.A.Rodríguez-Ortiza. (2014). Designing, processing and characterisation of titanium cylinders with graded porosity: An alternative to stress-shielding solutions. *Materials & Design*, *Volume 63*, 316–324.

7. FIGURE CAPTIONS

Figure 1. SEM microphotographs of all c.p.Ti surfaces. Images showed the different surfaces, with and without HF treatment as well the three different pore sizes of space holder (BA). Insets correspond to macroscopic images of the samples revealing the main differences (color and pore size and morphology) of the samples.

Figure 2. Pore's detail of cp. Ti samples by SEM. These microphotographs highlight the pores structure and the HF influence as surface modification treatment. Noticed am increased roughness at the microscale order as well as the presence of geometrical features (upper insets) due to HF treatment and PM process respectively.

Figure 3. Roughness quantification, Sa (μm) of c.p.Ti substrates by the analysis of confocal images using Sensomap software. A, B, C, and D correspond to the Sa values comparing flat and pores surfaces of A, B C and D surfaces at the three times of etching modification (0, 125, and 625). Upper and left insets showed clearly a bigger scale of flat surfaces. Noticed the higher affinity of chemical attack for pore surfaces which reached higher Sa values.

Figure 4. Cell viability of C2C12GFP cells at 1 day. Results were expressed as a percentage of D0 levels. All substrates showed similar metabolic activities with no statistical differences ($P \geq 0.05$).

Figure 5. Fluorescent microphotographs of cell adhesion and proliferation of C2C12-GFP premioblastic cell line. A) Cell attachment of D, DE, P and PE at1 day of cell incubation. All samples allowed cell attachment, noticing a slight increase in cell density in D0 which has not rough surface and no pores. Etched Ti scaffolds showed similar cell density as controls revealing the cell biocompatibility of the treatment. B) Cell proliferation of C2C12-GFP growing on D, DE, P and PE samples at 4 days of cell incubation. Noticed the increase of cell density showing the cytocompatibility character of the treatment.

Figure 6. Cell proliferation of MC3T3E1 preosteoblastic cells expressing cell metabolic activity results as relative fluorescence units at 4 and 7 days of cell culture (A and B respectively). These fluorescence levels showed similar cell proliferation as control and TCP. Noticed a slight reduction trend in porous samples of cell metabolic levels.

Figure 7. Microphotographs of cell morphology of osteoblast MC3T3E1 growing on all c.p. Ti samples at day 7. Actin fibers appeared in red and cell nuclei in blue due to Texas Red Phalloidin and Dapi staining. From these images, Ti samples achieved similar cell density covered the whole surface by preosteoblast showing the cytocompatibility character of the samples.

Figure 8. Evaluation of cell differentiation at 7 days. Detection of Alkaline phosphatase enzyme (ALP), an earlier bone marker, on osteoblast growing on cp. Ti samples. The higher ALP levels were observed in 625 HF treatment and in the pore of bigger size B and C.

Figure 9. Evaluation of cell mineralization at 14 days. Microphotographs of calcium deposits in red color after alizarin test. The higher calcium deposits were increased on B and C samples with 125 HF treatment.

Figure 10. RAW 264.7 seeded on titanium implants with different porosity and roughness. A. Samples of titanium implants (D without porosity and A with porosity; 0s of chemical attack without roughness and 625s of chemical attack with roughness). B. Actin fibers, cell nuclei by Hoechst staining, and M1 cell surface marker (CCR7) staining at 48h. Cells growing on D0 (without porosity and roughness) presented an increased polarization of M1 that was corroborated with the positive signal of CCR7 staining. Moreover, some multinucleated cells, that could differentiate into FBGC (see yellow arrows), were observed on these samples. In contrast, D625 and A625s, as well as A0, showed less M1 polarization compared to D0 revealing the positive effects of both parameters roughness and porosity on the control of immune response.

Figure 1

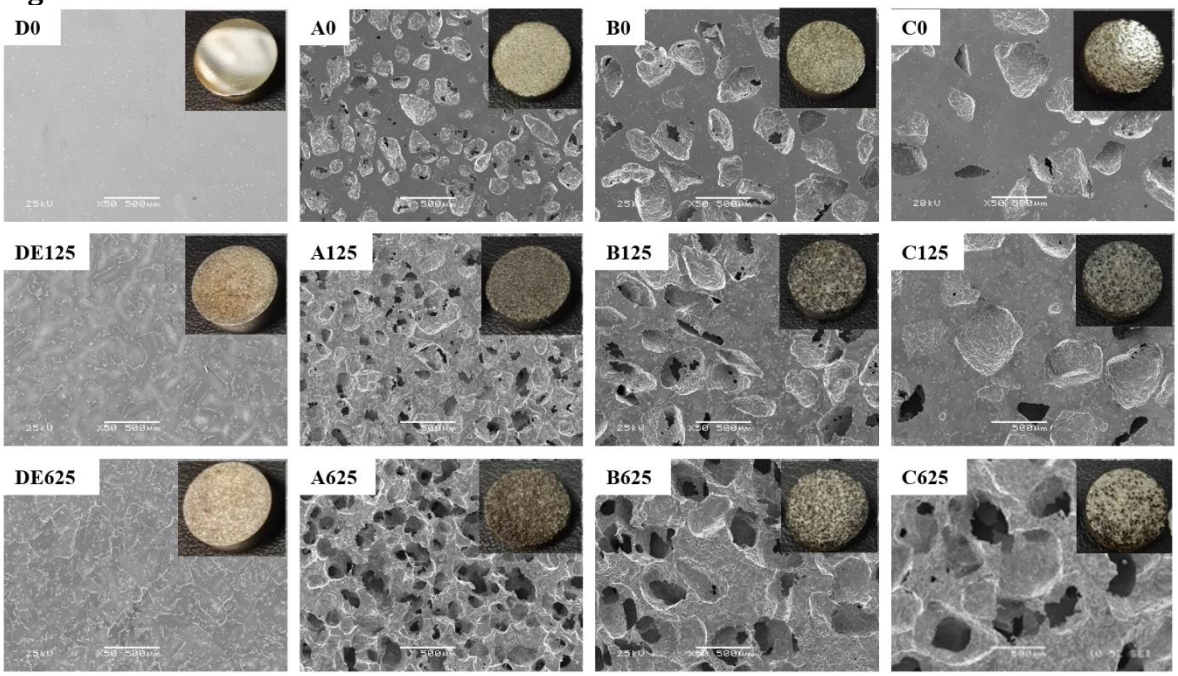

Figure 2

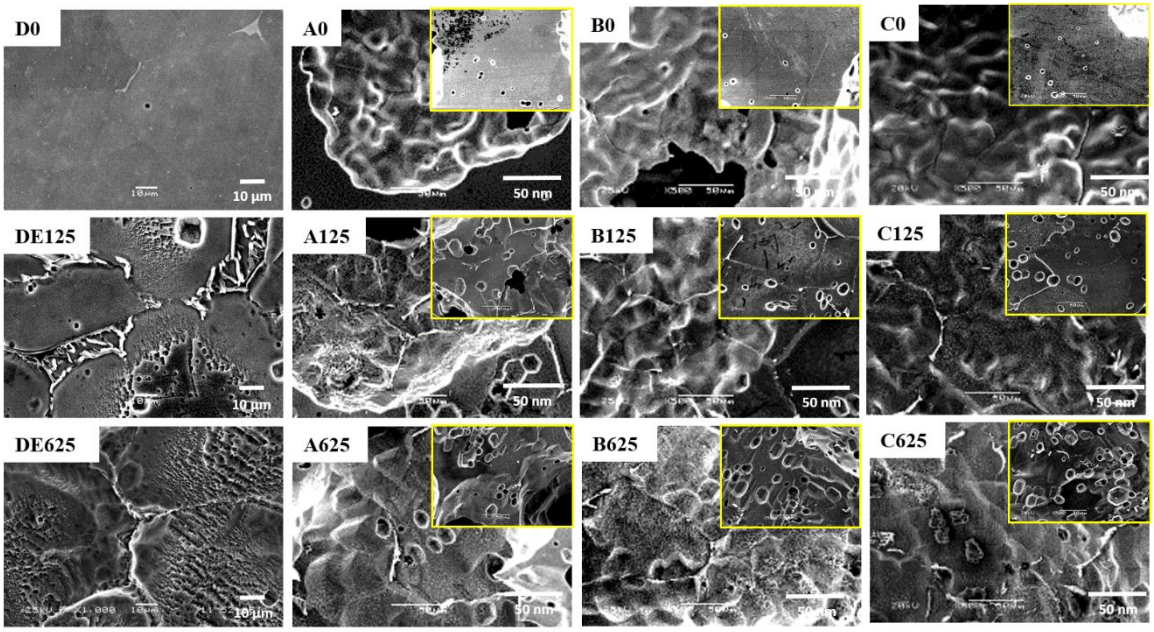

Figure 3

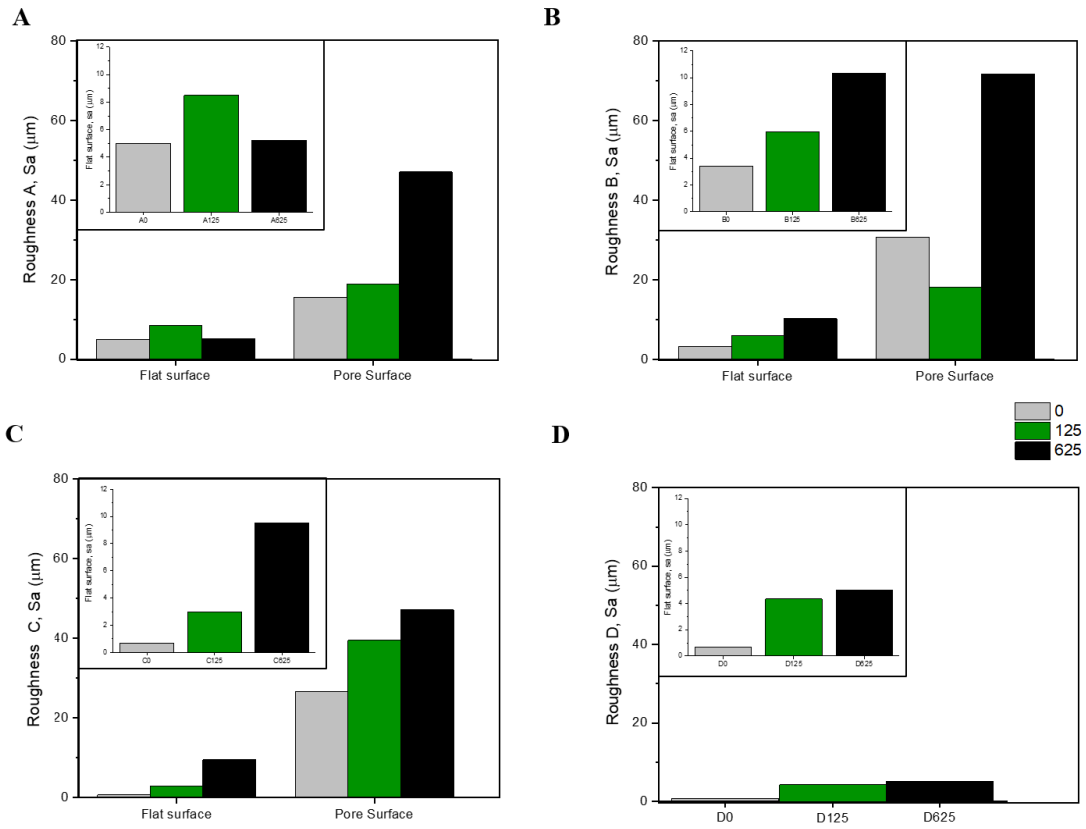
A
B
C
D
Roughness A, Sa (μm)
Roughness B, Sa (μm)
Roughness C, Sa (μm)
Roughness D, Sa (μm)
Flat surface
Pore Surface
0
125
625
D0
D125
D625

Figure 4

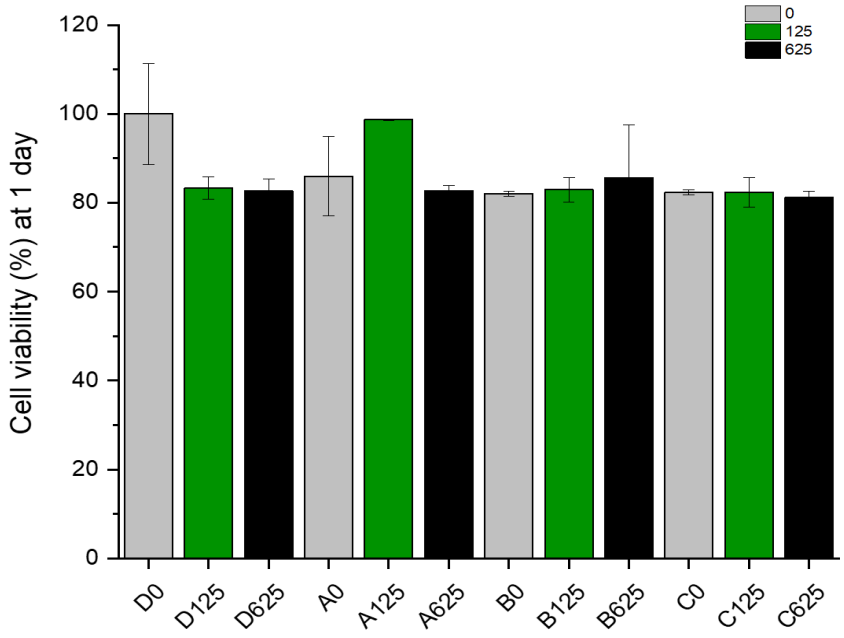
0
125
625
Cell viability (%) at 1 day
120
100
80
60
40
20
0
D0
D125
D625
A0
A125
A625
B0
B125
B625
C0
C125
C625

Figure 5

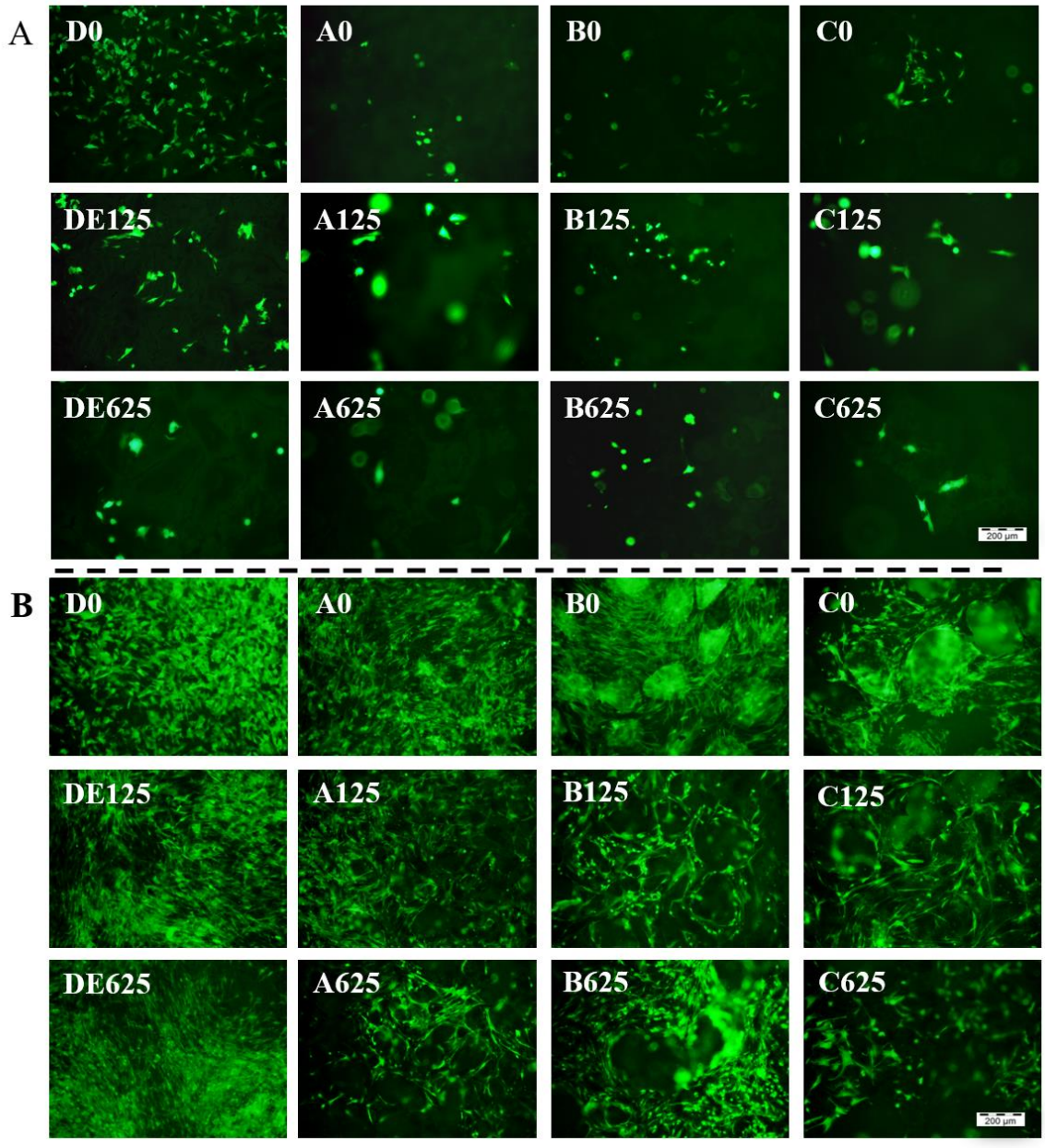
A
D0
A0
B0
C0
DE125
A125
B125
C125
DE625
A625
B625
C625
200 μm
B
D0
A0
B0
C0
DE125
A125
B125
C125
DE625
A625
B625
C625
200 μm

Figure 6

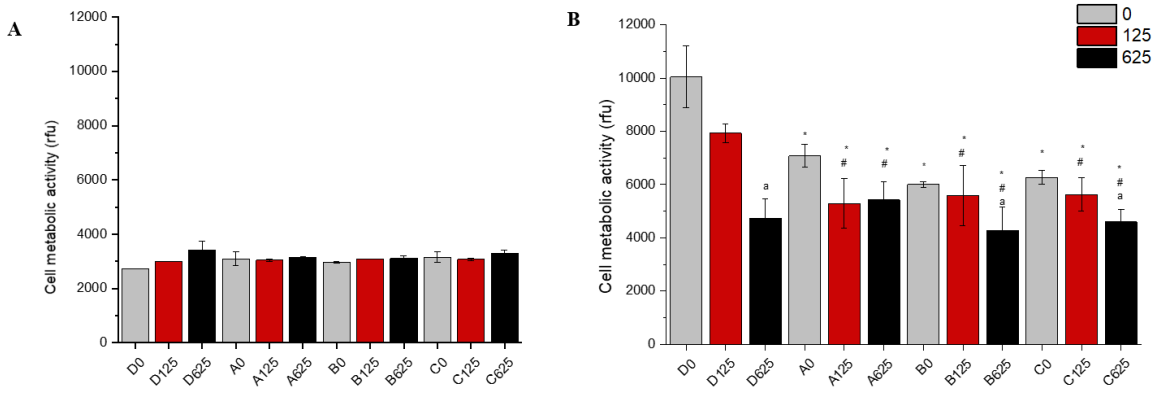

Figure 7

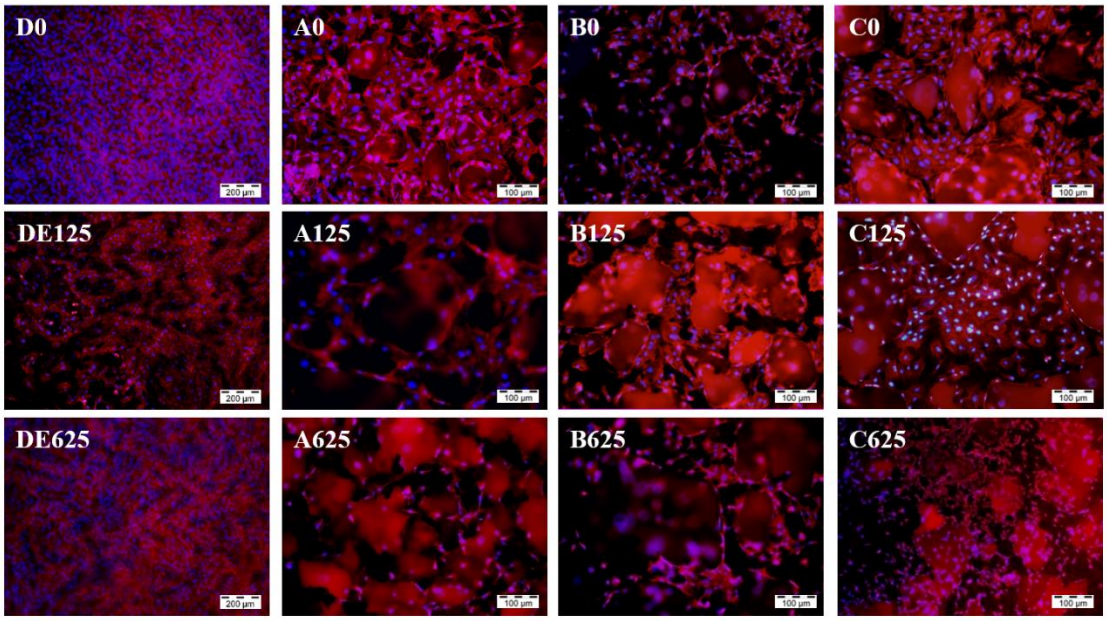

Figure 8

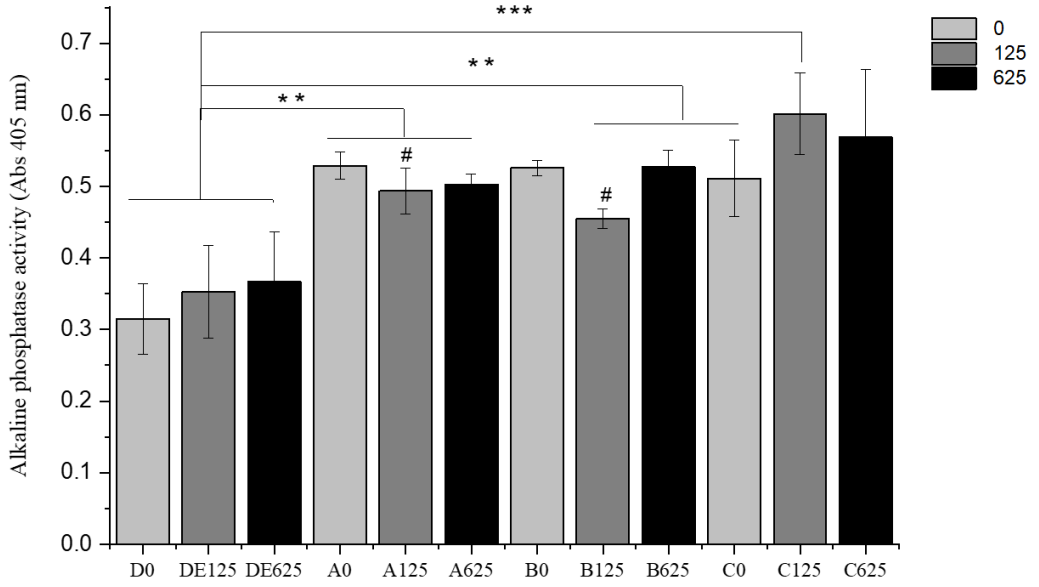

Figure 9

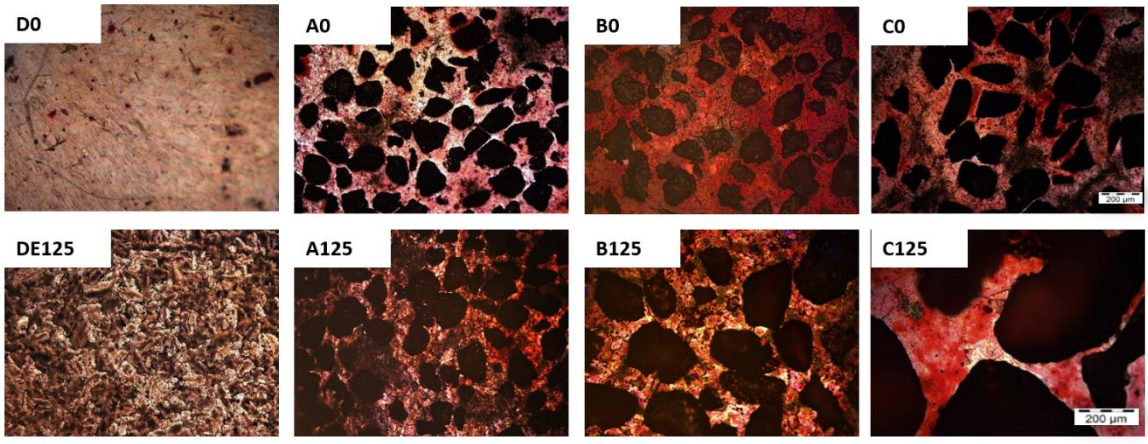

Figure 10

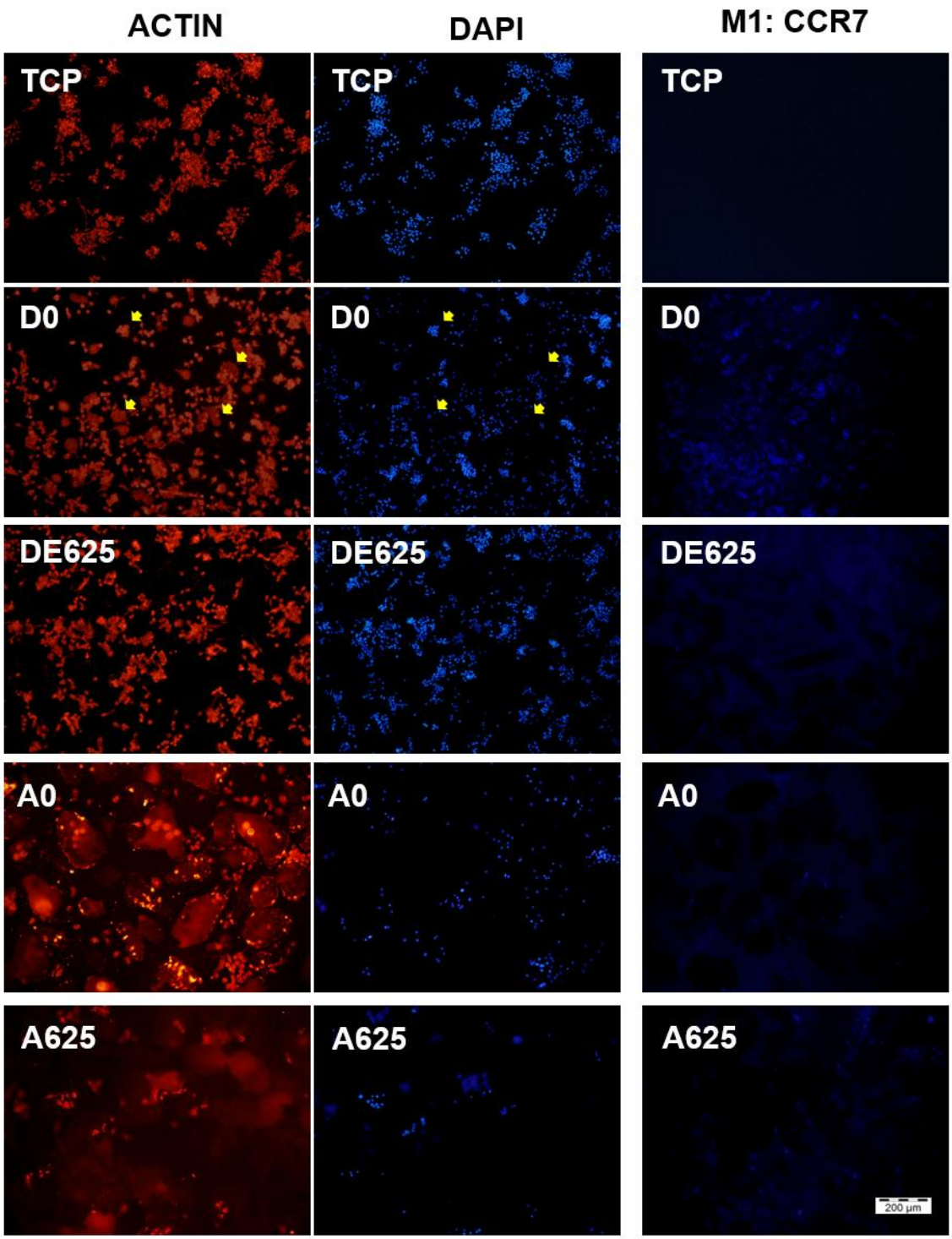
ACTIN
DAPI
M1: CCR7
TCP
TCP
TCP
D0
D0
D0
DE625
DE625
DE625
A0
A0
A0
A625
A625
A625
200 µm

Figure S1

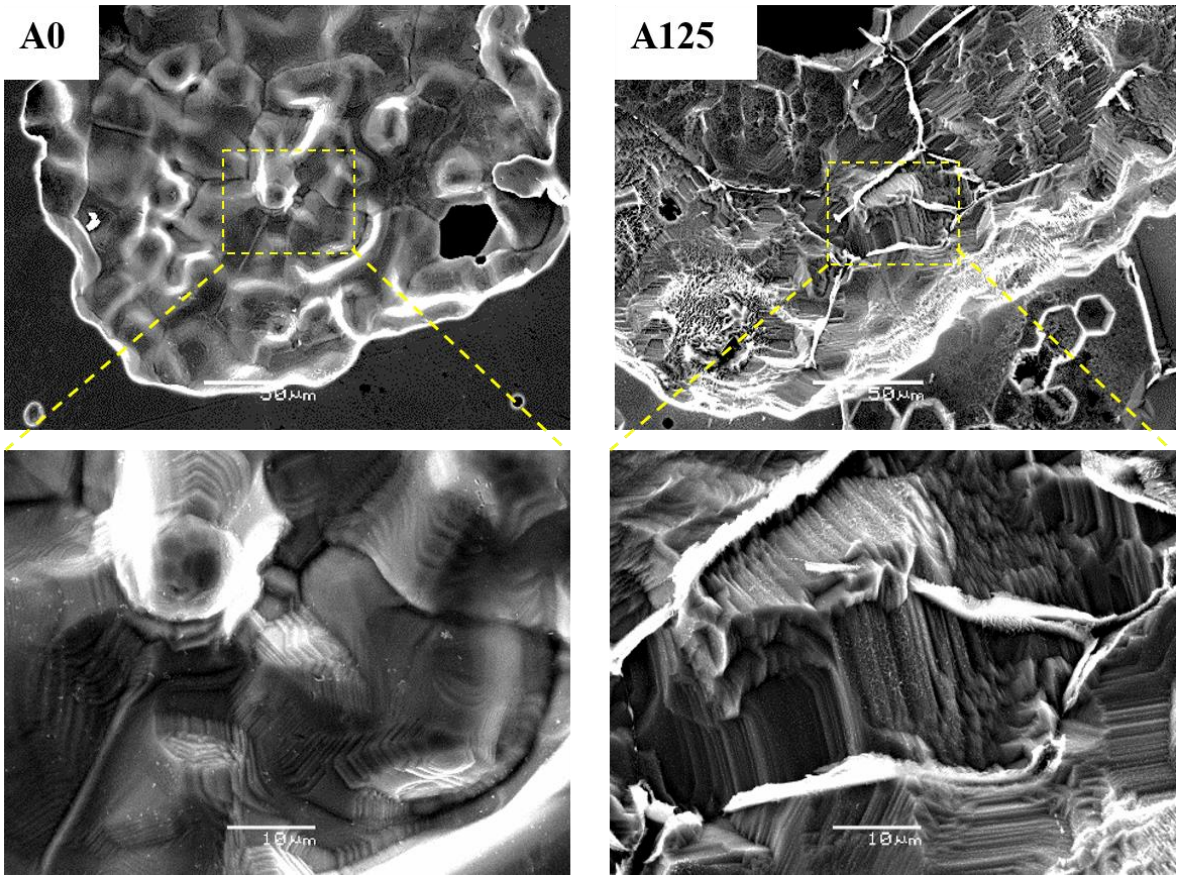

4. CONCLUSIONES GENERALES

- En este trabajo se ha logrado implementar un tratamiento químico que modifica la porosidad de los estratos de Ti c.p poroso, además de generar un nuevo patrón de micro rugosidad adicional que no se esperaba mediante el uso de un inhibidor orgánico. Este tratamiento químico modificó la superficie y la porosidad de los mismos en términos de fracción de volumen y topografía.

- Los sustratos porosos experimentaron variaciones microestructurales y topográficas, las cuales implicaron una disminución de las propiedades mecánicas de los sustratos, obteniendo valores cercanos a los del hueso cortical y de esta manera confirmado su uso como matrices de Ti poroso biomiméticos.

- Con este estudio se logra correlacionar la viabilidad celular, adhesión, proliferación, morfología celular y la respuesta inmune de las células premioblásticas, preosteoblásticas y macrófagos. La rugosidad mejoró la diferenciación celular y controló la respuesta inmune para reducir el fenotipo M1. Las muestras con tiempo de tratamiento 0s y 125s favorecieron la biocompatibilidad de las muestras, mientras que las muestras con el tratamiento químico de 625s mejoraron los procesos de diferenciación de osteoblastos.

- La evaluación in vitro de muestras de Ti porosas no es suficiente para determinar el grado de osteointegración de las muestras; haciendo necesarios estudios in vivo con modelos animales que permitan una mejor comprensión de los procesos de osteointegración en el entorno complejo.

- El alto valor agregado que le darán la modificaciones superficiales a implantes de Ti poroso conllevaría a la sustitución de otras aleaciones costosas a base Cr-Co, y a la reducción de la importación de implantes contribuyendo a la disminución de sus costos y de los tratamientos, tanto para el paciente como para las entidades hospitalarias. Además, la proyección a nivel industrial de la prestación de los servicios de este tipo de tratamientos impactará positivamente a las empresas colombianas fabricantes y/o comercializadoras de implantes dentales haciéndolas más productivas y competitivas.

- Este tipo de estudios hace un aporte significativo al desarrollo e investigación biomédico en el área de desarrollo de nuevos biomateriales; fortaleciendo de esta manera el nivel científico, investigativo y académico mediante el uso de tratamientos superficiales convencionales en Ti poroso, dando como resultado una novedosa topografía superficial que permitiría mejorar la osteointegración del implante al hueso.

- Con el desarrollo de nuevas topografías sobre implantes fabricados en Ti poroso se pretende incrementar la vida útil de los mismos, mejorar su biocompatibilidad y su osteintegración disminuyendo los riesgos de aflojamiento, rechazo, infecciones y otras enfermedades de los pacientes durante las intervenciones quirúrgicas y tiempos postoperatorios, reduciendo además los costos de tratamiento.

- Con el desarrollo de biomateriales innovadores, se puede consolidar conocimientos en la industria biomédica nacional e internacional. Teniendo en cuenta que en Colombia el avance en este tipo de técnicas se encuentran en proceso de desarrollo e investigación y con muy bajo nivel de publicación científica.

- Este trabajo permitió fortalecer vínculos científicos y la colaboración académica entre el grupo de investigación BAMR de la Universidad de Antioquia, el grupo de estudios biofuncionales de la Universidad Complutense de Madrid, la Universidad CES, la universidad de Sevilla y la Universidad de illinois. .

5. BIBLIOGRAFÍA

Andrés O. Garzón, Nelly O, Aguirre, & Jhon J Olaya. (2013). Estado del arte en biocompatibilidad de recubrimientos. *Visión Electrónica*, *Volumen:7*, pág: 160–177.

Angel Coronel. (2015). *Surface Modification of Porous Titanium for Bone Repair: Controlled Etching and Deposition of Bioactive Composite Coatings by EPD Technique* (Pregrado). Universidad de Sevilla.

C. Aparicio. (2004). *Tratamientos de superficie sobre Ti Cp para la mejora de osteointegración de los implantes dentales.* Universidad Politecnica de Cataluña.

Crowninshield, R.D., Rosenberg, A.G., & Sporer, S.M. (2006). Changing demographics of patients with total joint replacement. *Clinical Orthopaedics and Related Research*, 266–272.

J.M Macak, H Tsuchiya, , A. Ghicov, K. Yasuda, R. Hahn, & S. Bauer. (2007). TiO2 nanotubes: Self-organized electrochemical formation, properties and applications, *11*(1–2,), Pages 3-18.

Juan Pavón. (2006). *Fractura y fatiga por contacto de recubrimientos de vidrio sobre Ti6Al4V para aplicaciones biomédicas*. Universitat

Politècnica de Catalunya. Departament de Ciència dels Materials i Enginyeria Metal·lúrgica.

Kanazawa I, Yamaguchi T, Yano S, Yamahuchi M, Yamamoto M, & Sugimoto T. (2007). Adiponectin and AMP kinase activator stimulate proliferation, differentiation, and mineralization of osteoblastic MC3T3-E1 cells. *BMC Cell Biology*, *8: 51*.

M. Niinomi, & M. Nakai. (2011). Titanium-Based Biomaterials for Preventing Stress Shielding between Implant Devices and Bone. *Internacional Journal of Biomaterials*, 1–10.

M. Vandrovcova1, 1, & L. Bacakova. (2011). Adhesion, growth and differentiation of osteoblasts on surface-modified materials developed for bone implants. *Physiol Res. ., ;60(3):*, 403-17.

Ministerio de salud y porteccion Social. Colombia. (2015). IV Estudio Nacional de Salud Bucal. ENSAB IV. Situación en salud Bucal. Retrieved from https://www.minsalud.gov.co/sites/rid/Lists/BibliotecaDigital/RIDE/VS/PP/ENSAB-IV-Situacion-Bucal-Actual.pdf

N. Sumitomo, K. Norikate, & T. Hattori. (2008). Experiment study on fracture fixation with low rigidity titanium alloy: plate fixation of tibia fracture model in rabbit. *Journal of Materials Science, 19. No. 4*, 1581–1586.

Robinson Montes. (2013). *Desarrollo de nuevas superficies de Ti vìa electroquìmica para implantes dentales.* Universidad de Antioquia.

Y torres, J. Pavon, & JA Rodriguez. (2012). Processing and characterization of porous titanium for implatns. *Journal of Materials Processing Technology*, 1061–1069.

Y. Torres, J.A Rodriguez, J.Pavón, S. Arias, M. Echeverry,, S. Robledo, & V. Amigo. (2012). Processing, characterization and biological testing of porous titanium obtained by space-holder technique. *J Mater Sci.*, 6565-76.

Yadir Torres, Sheila Lascano, Jorge Bris, Juan Pavon, & Jose A Rodriguez. (2014). Development of porous titanium for biomedical applications: A comparison between loose sintering and space holder techniques. *Materials Science and Engineering C 37*, 148–155.

Y.Torres, P.Trueba, J.Pavón, I. Montealegre, & J.A.Rodríguez-Ortiza. (2014). Designing, processing and characterisation of titanium cylinders with

graded porosity: An alternative to stress-shielding solutions. *Materials & Design, Volume 63*, 316–324.